Exchange-spring systems: Coupling of hard and soft ferromagnets as measured by magnetization and Brillouin light scattering (invited)

M. Grimsditch[a)]
Materials Science Division, Argonne National Laboratory, Argonne, Illinois 60439

R. Camley
Physics Department, University of Colorado, Colorado Springs, Colorado 80933-7150

E. E. Fullerton
Materials Science Division, Argonne National Laboratory, Argonne, Illinois 60439 and IBM Almaden Research Center, San Jose, California 95120-6099

S. Jiang, S. D. Bader, and C. H. Sowers
Materials Science Division, Argonne National Laboratory, Argonne, Illinois 60439

An experimental and theoretical study is presented of the normal magnetic modes in spiral ferromagnetic structures. The bilayer system studied consists of Fe layers (25, 50, 100, and 200 Å thick) that are exchange coupled to 200 Å thick SmCo films that have ≈200 kOe anisotropies. The Fe spiral—induced by an external magnetic field that is applied opposite to the direction of the magnetized film—results in a structure similar to that encountered in a Bloch domain wall. The magnetization and the field dependence of the magnons in various Fe films are explained by the theoretical model. [S0021-8979(99)47008-2]

I. INTRODUCTION

Exchange-spring magnets are two-phase materials composed of hard and soft magnetic grains. It is likely that for technological applications these materials will be in the form of nanodispersions of the two phases;[1,2] however, there is also considerable effort aimed at understanding their properties in thin-film form.[3–11] Such investigations should improve our fundamental understanding of the exchange-spring mechanism. In a recent study[11] a detailed characterization of such films was presented based mainly on magnetization measurements, although some Brillouin scattering data on the frequency of the magnon mode was included. A simple model was used to describe the magnon behavior in the aligned magnetic state, but to explain the behavior in the spiral state it was indicated that a full theoretical analysis would be necessary. In the present work we present a more complete theoretical and experimental study of the excitations in the spiral and aligned states.

Experimental magnon frequencies in SmCo/Fe bilayers are reported herein for Fe films with thicknesses between 25 and 200 Å deposited on SmCo films of fixed thickness of 200 Å. Details of the deposition conditions are given in Ref. 11. The films are epitaxially grown on MgO(100) utilizing a Cr buffer layer. The hexagonal SmCo is *b*-axis oriented with the magnetically easy *c* axis in the film plane, which defines the uniaxial direction. The Brillouin spectra were recorded utilizing a five-pass Fabry–Pérot interferometer. The method used to calculate the magnon frequencies follows the general lines given in Ref. 12. The manner in which the minimum-energy configuration of the Fe spins is obtained leads, in a straightforward manner, to the frequency of the magnon modes. All features observed experimentally in both the magnetization and the magnon frequencies are reproduced quantitatively by the model.

II. THEORETICAL DEVELOPMENT

A schematic diagram of our model is shown in Fig. 1(a). Each arrow corresponds to the total spin of a given atomic layer. The larger arrows for Fe indicate that its magnetization is greater than that of SmCo. The model also assumes that the SmCo spins are subjected to an anisotropy field of ≈200 kOe, while the anisotropy in the Fe layers is small. The exchange coupling between atomic layers is given by $AJ_i \cdot J_{i+1}$, with A appropriate for Fe or SmCo, as the case might be, and an average A is used to describe the SmCo/Fe inter-

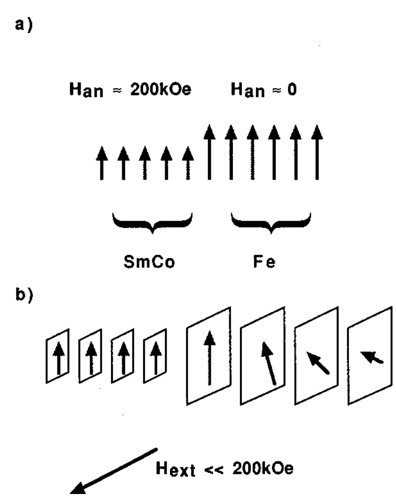

FIG. 1. (a) Schematic diagram of SmCo/Fe bilayer. (b) Diagram of the spiral structure induced in the Fe layer by a external field perpendicular to the magnetization.

[a)]Electronic mail: marcos.grimsditch@qmgate.anl.gov face. Figure 1(b) exemplifies the spin configuration when an external field is applied perpendicular to the easy axis.

This simple model, with a single set of parameters, was found[11,13] to produce excellent agreement with the measured magnetization along the in-plane hard and easy axes for the samples investigated. However, the switching field of the SmCo layer was not well reproduced; this is probably due to a switching mechanism involving domain formation, which is not included in the model.

We use a single numerical scheme to find both the equilibrium spin configuration and the spin wave frequencies. One begins by writing the coupled equations of motion for the spins in each atomic layer. The system is then given some initial configuration and allowed to evolve in time according to the equations of motion. At the beginning the damping term is set quite high and, thus, the system evolves into a structure wherein the spins within each layer point along their local effective-field direction. This essentially locates the minimum-energy state. The damping is then reduced substantially and the system is given a small perturbation. Again the system is allowed to evolve in time and one finds $m_x(t)$, $m_y(t)$, and $m_z(t)$ for each layer. The Fourier transform of the time-dependent magnetizations then gives the spin wave frequencies.

As we will see, modeling the system as a set of interacting layers does a good job of explaining both the static data (hysteresis curves) and the dynamic results (spin wave frequencies). The total energy density of the system may be written[1]

$$E=-\sum_{i=1}^{N-1}\left(\frac{A_{i,i+1}}{d^2}\right)\mathbf{a}^{(i)}\cdot\mathbf{a}^{(i+1)}-\sum_{i=1}^{N}K_i(a_z^{(i)})^2 -\sum_{i=1}^{N}(\mathbf{H}+\mathbf{h}^{(i)})\cdot\mathbf{a}^{(i)}\mathbf{M}^{(i)}. \quad (1)$$

Here $\mathbf{M}^{(i)}$ is the magnetization vector in layer i, K_i is the anisotropy constant for layer i, and $A_{i,i+1}$ is the exchange coupling constant between layers i and $i+1$. The quantity $\mathbf{h}^{(i)}$ is a small fluctuating magnetic field arising from the dipole field of the precessing spins. The distance between magnetic layers is d. For convenience, we have changed to unitless variables for the magnetization, i.e., $\mathbf{a}^{(i)}=\mathbf{M}^{(i)}/\mathbf{M}^{(i)}$.

We start with the Bloch equations of motion for the spin system. The equations of motion for layer i are given by

$$\frac{d\mathbf{a}^{(i)}}{dt}=\gamma\mathbf{a}^{(i)}\times\mathbf{H}_{\text{eff}}+\left(\frac{\alpha}{M^{(i)}}\right)\mathbf{a}^{(i)}\times\mathbf{a}^{(i)}\times\mathbf{H}_{\text{eff}}. \quad (2)$$

In Eq. (2) the first term on the right represents the torque produced on a spin in layer i by an effective magnetic field. The second term is the Landau–Lifshitz damping term which allows the spin to decay to the local-field direction, but keeps the magnitude of the spin constant. Here γ is the gyromagnetic ratio and α is the effective damping parameter. $\mathbf{H}_{\text{eff}}$ is the effective field acting on layer (i) defined using Eq. (1):

$$\mathbf{H}_{\text{eff}}=-\partial E/\partial\mathbf{M}^{(i)}. \quad (3)$$

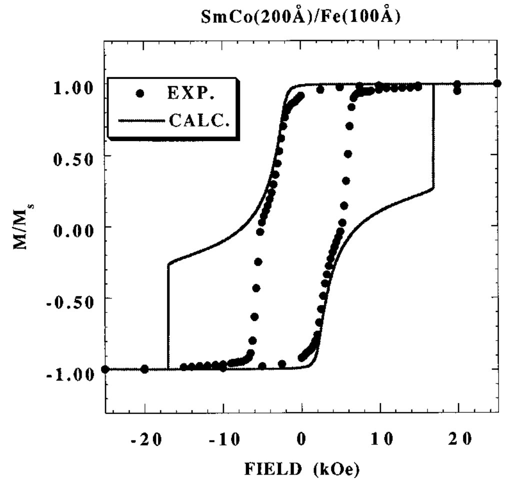

FIG. 2. Magnetization loop for the 100 Å Fe film on 200 Å SmCo. The symbols are experimental data, the full line is the model calculation.

The total effective field is a sum of exchange, anisotropy, dipolar, and external fields. We assume that the main contribution to the dipole field **h** is the demagnetizing field of a thin layer acting on itself; thus, $\mathbf{h}=4\pi Ma_y$. This approximation works well for thin films in the long wavelength limit where $qD\ll 1$, where D is the thickness of the film and q is the component of the spin wave wave vector parallel to the surface. For typical Brillouin scattering experiments this approximation gives reasonable results for thicknesses on the order of a couple of hundred Å or less.

Once the coupled equations of motion for all the layers are obtained, the equations are numerically integrated forward in time using a second-order Runge–Kutta scheme. The parameters used in the calculation are those given in Ref. 11, i.e., $A_{i,i+1}=1.2\times10^{-6}$ erg/cm for SmCo, $A_{i,i+1}=2.8\times10^{-6}$ erg/cm for Fe, $K_i=5\times10^7$ erg/cm^3 for SmCo, $K_i=10^3$ erg/cm^3 for Fe, $M_s=550$ emu/cm^3 for SmCo, and $M_s=1700$ emu/cm^3 for Fe. The gyromagnetic ratio is taken to be 2.92 GHz/kOe, the value appropriate for Fe. We take α/γ to be 200 G, a reasonable value for metallic systems. We emphasize that there are no parameters in the calculations that have been adjusted to fit the experimental frequencies.

III. RESULTS AND DISCUSSION

The magnetization of our samples was investigated extensively in Ref. 11. For completeness the magnetic loop with the field along the easy axis for our 100 Å Fe sample is given in Fig. 2. The symbols are experimental data and the full line is the result of the calculations described in Sec. II. Again, note that except for the switching field of the SmCo layer, excellent agreement is obtained. The transverse magnetization is also reproduced by the model and is shown in Refs. 11 and 13.

Brillouin spectra were recorded with the applied field H along both the easy and hard axes of the SmCo. By symmetry it is clear that for fields along the hard axis, the results are the same for positive or negative fields; we therefore measured magnon frequencies for only one of the field directions. Hard-axis magnon frequencies are plotted as open

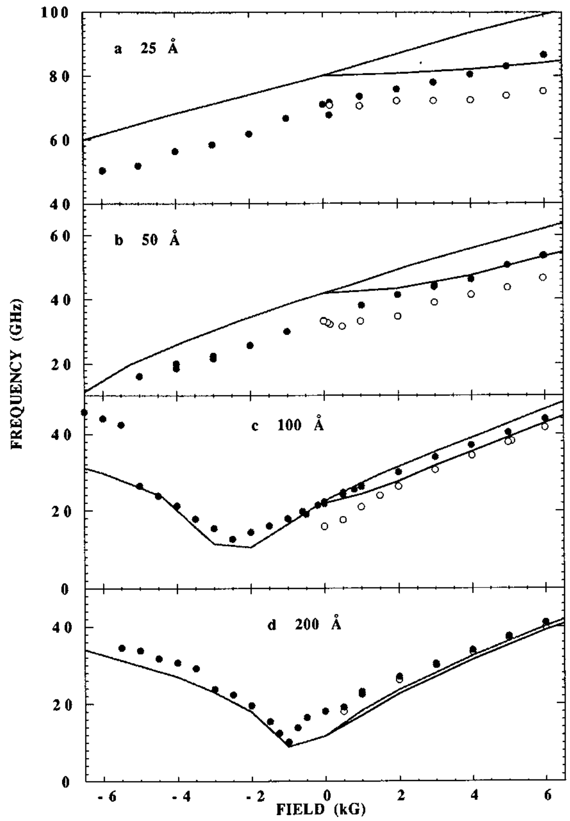

FIG. 3. Measured Brillouin frequencies along the easy (full) and hard (open) axes of SmCo/Fe bilayers. The full lines are the model calculations. Sections a, b, c, and d correspond to Fe thicknesses 25, 50, 100, and 200 Å, respectively.

symbols in Figs. 3 and 4. When the field is applied along the easy axis (full symbols in the figures) the positive and negative fields are no longer equivalent. We define the positive direction as that of the magnetization of the SmCo underlying film. In Fig. 3 we present the Brillouin results for four samples; the full lines represent the theoretical calculations, as described in Sec. II. For the 25 and 50 Å samples the fields attainable were not sufficient to reach the switching field of the underlying SmCo layer. The clearest data were

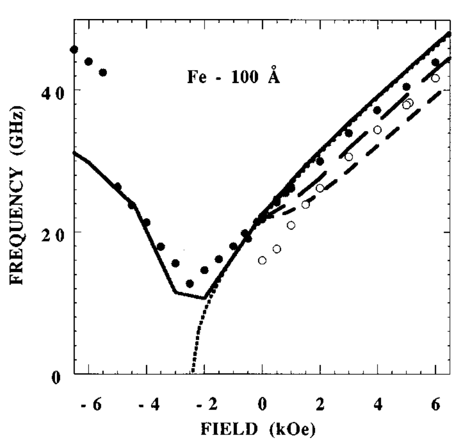

FIG. 4. Expanded view of Fig. 3(c) which also includes the predictions of the full calculation (full and long dashes) and approximate calculation (dotted and short-dashed lines).

obtained for the 100 Å sample, so this sample was chosen for a detailed comparison with the calculations.

The comparison of experiment and theory is shown in Fig. 4. The full and long-dashed line are the full calculations for easy and hard axes; the dotted and short dashed lines will be described below. The data for the field along the easy axis increase monotonically for positive fields, but show an initial decrease as the field decreases below zero. At $H_0 = -2.5$ kOe there is a frequency minimum which coincides with the onset of decreasing magnetization (Fig. 2) indicating the reorientation of the Fe film into a spiral structure, as shown in Fig 1(b). As the field is made more negative, the frequency increases; this corresponds to a region in which the pitch of the spiral is increasingly compressed toward the Fe/SmCo interface. Finally, at $H_0 = -5$ kOe, there is a jump in the measured frequency corresponding to the reversal of the magnetization of the underlying SmCo. Below this field the experimental frequencies are the same as for positive fields. The calculated frequencies, since the model does not account for the SmCo switching, do not agree with the measured ones below -5 kOe.

We stress that the calculations reproduce both the hard-axis frequencies as well as the easy-axis results for -5 kOe $H_0 < -2.5$ kOe. Since these calculations use the spiral ground-state configuration as a basis for the excitation frequencies, the good agreement between theory and experiment provides strong support both for the existence of the spiral configuration and that the model correctly describes the SmCo/Fe bilayer.

Since there are no adjustable parameters in the theory, the overall agreement between theory and experiment for all Fe thicknesses is gratifying. The most significant discrepancies between theory and experiment in Figs. 3 and 4 are: the absence of switching of the underlying SmCo layer in the theory, the overall lower values of the experimental frequencies, and that at zero field the calculated frequencies are equal while the measured ones are not. The switching field problem is due to the simplicity of the model which only allows switching by a coherent rotation of spins. The average frequency difference between calculation and experiment could easily be remedied by slight modifications in the material parameters, most notably a slight reduction in the magnetization of Fe or the inclusion of a perpendicular anisotropy. However, the fact that the experimental frequencies at zero field are different for easy and hard directions is clear evidence that the approximation $qD \ll 1$ is inadequate; the reduction in the hard–easy difference for the thinner Fe films is consistent with this explanation. Furthermore, since the finite q correction term enters only when q is perpendicular to M, it also provides an explanation of why in Fig. 3(c), as the magnetization with the field along the hard direction rotates away from the direction of q, the qD correction term becomes comparable for both orientations and the measured frequency difference between hard and easy axes is reduced. In Summary, the difference between the hard- and easy-axis data depends on the interplay between an average anisotropy induced by the underlying SmCo, which scales as $\approx 1/D$, and the finite q correction term, which scales as D, but which also depends on how much the magnetization is rotated.

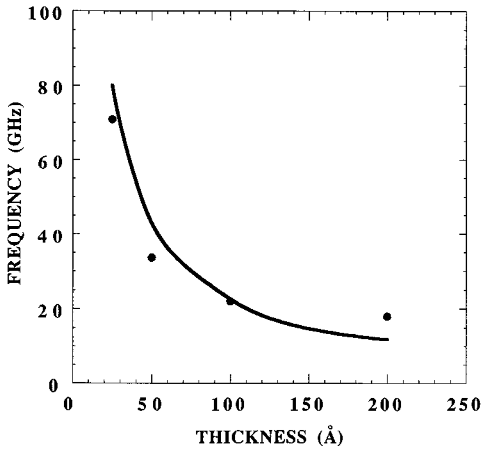

FIG. 5. Zero field Brillouin frequencies vs Fe thickness. Symbols are experimental, the full line is calculated.

Although the theory produces good overall agreement with experiment, the calculations require considerable computational effort. It is therefore instructive to investigate the validity of the simpler model introduced *ad hoc* in Ref. 11, and which also yielded a reasonable description over a limited field range. That model treated the system as an Fe film with an effective anisotropy induced by the substrate. It is well known that the resonance frequency in a thin film can be approximated by

$$\omega=\gamma\sqrt{H_0(H_0+4\pi M)}. \qquad (4)$$

If we consider measurements along the easy axis, where the Fe and SmCo magnetizations are parallel to the applied field, it is reasonable to replace H_0 in Eq. (4) by H_0+H_{ex}, i.e., the exchange biasing field is simply added to the external field. With $H_{ex}=2.4$ kOe, this gives an excellent fit (dotted line in Fig. 4) to the easy-axis data down to -2.5 kOe, where the spiral state is induced. When the external field is directed along the hard axis, we assume that H_{ex} still points along the easy axis, so H_0 and H_{ex} are now perpendicular. The total field is now given by

$$H_{total}=\sqrt{H_0^2+H_{ex}^2}, \qquad (5)$$

and when this is substituted in Eq. (4) we get the short-dashed line shown in Fig. 4. This describes the qualitative behavior reasonably well, but fails to yield the correct value for the shift between the easy- and hard-axis results. This very simple approach provides a qualitative description of the excitation frequencies provided that the Fe layer is not in the twisted state. For the thinnest Fe films, where one does not expect much of a twist, the simple model outlined above agrees well with both the full theoretical calculations and the experiments.

A final experimental observation is the overall frequency increase of the zero-field frequency as the Fe thickness is decreased. In Fig. 5 we plot the zero-field frequency for all four samples (full symbols). The behavior can be qualitatively understood as resulting from the contribution of the exchange coupling at the interface. The results are quantitatively reproduced by the full calculation (full line).

IV. CONCLUSIONS

The magnon frequencies in SmCo/Fe bilayers, with different thicknesses of the Fe layer, have been measured using Brillouin scattering. The frequencies measured for fields applied along the hard and easy axes are well reproduced by a simple one-dimensional model. The good agreement between theory and experiment, which extends to the magnetization loops, provides strong evidence that the microscopic origin of spring magnets is well understood.

ACKNOWLEDGMENTS

Work at Argonne supported by the US DOE Basic Energy Sciences-Materials Sciences under Contract No. W-31-109-ENG-38. Work at Colorado Springs supported by ARO Grant No. DAAG55-98-0294.

[1] E. F. Kneller and R. Hawig, IEEE Trans. Magn. **27**, 3588 (1991).
[2] J. M. D. Coey, Solid State Commun. **102**, 101 (1997).
[3] R. Skomski, Phys. Rev. B **48**, 15812 (1993).
[4] E. E. Fullerton, C. H. Sowers, J. P. Pearson, S. D. Bader, X. Z. Wu, and D. Lederman, Appl. Phys. Lett. **69**, 2438 (1996).
[5] K. Mibu, T. Nagahama, and T. Shinjo, J. Magn. Magn. Mater. **163**, 75 (1996).
[6] D. Givord, J. Betz, K. Mackay, J. C. Toussaint, J. Voiron, and S. Wünchner, J. Magn. Magn. Mater. **159**, 71 (1996).
[7] S. Wünchner, J. C. Toussaint, and J. Voiron, Phys. Rev. B **55**, 11576 (1997).
[8] Y. Suzuki, R. B. van Dover, E. M. Gyorgy, J. M. Phillips, and R. J. Felder, Phys. Rev. B **53**, 14016 (1996).
[9] I. A. Al-Omari and D. J. Sellmyer, Phys. Rev. B **52**, 3441 (1995).
[10] M. Shindo, M. Ishizone, H. Kato, T. Miyazaki, and A. Sakuma, J. Magn. Magn. Mater. **161**, L1 (1996).
[11] E. E. Fullerton, J. S. Jiang, M. Grimsditch, C. H. Sowers, and S. D. Bader, Phys. Rev. B **58**, 12193 (1998).
[12] R. J. Astalos and R. E. Camley, Phys. Rev. B **58**, 8646 (1998); R. E. Camley and R. J. Astalos, J. Magn. Magn. Mater. (in press).
[13] J. S. Jiang, E. E. Fullerton, M. Grimsditch, C. H. Sowers, and S. D. Bader, Proceedings of the 43 Annual Conference on Magnetics and Magnetic Material, San Francisco, CA, 1998.